Dynamics of soluble gas exchange in the airways III. Single-exhalation breathing maneuver

STEVEN C. GEORGE, ALBERT L. BABB, AND MICHAEL P. HLASTALA
Departments of Chemical Engineering, Medicine, and Physiology and Biophysics, University of Washington, Seattle, Washington 98195

GEORGE, STEVEN C., ALBERT L. BABB, AND MICHAEL P. HLASTALA. *Dynamics of soluble gas exchange in the airways. III. Single-exhalation breathing maneuver.* J. Appl. Physiol. 75(6): 2439–2449, 1993.—The exchange characteristics of a highly soluble gas with the pulmonary airways during a single-exhalation maneuver were analyzed using a mathematical model previously described by our group (M. E. Tsu et al. *Ann. Biomed. Eng.* 16: 547–571, 1988). The model integrates the simultaneous exchange of water, heat, and a soluble gas with the pulmonary airways. The purpose of this paper is to provide experimental data for model validation. Exhaled ethyl alcohol concentration profiles of human subjects were measured with an Intoxilyzer 5000 and were plotted against exhaled volume measured with a wedge spirometer. Each subject performed a series of breathing maneuvers in which exhalation flow rate was the only variable. Phase III has a positive slope (0.047 ± 0.0089 mol alcohol in air · mol alcohol in alveolus^{-1} · l^{-1}) that is statistically independent ($P > 0.05$) of flow rate. Reducing the molecular diffusion coefficient of alcohol in the nonperfused tissue layer improves the fit of the model to the experimental data. The optimal diffusion coefficient of alcohol for all subjects was 12 ± 5.3 (SD) $\times 10^{-7}$ cm^2/s, which is 8% of the diffusion coefficient of alcohol in water (1.6×10^{-5} cm^2/s). We concluded that the experimental data showing a positive slope of the exhaled alcohol profile are consistent with a reduced diffusivity of alcohol in the respiratory mucosa. The reduced diffusion coefficient enhances reabsorption of alcohol by the airways on exhalation and creates a positive phase III slope.

mathematical model; diffusion coefficient; alcohol breath test; phase III slope

GAS EXCHANGE EFFICIENCY is extremely dependent on the blood-air partition coefficient (λ_b) of the gas. The major effort in respiratory physiology over the past 40 years has been to characterize the exchange of gases with low ($\lambda_b < 0.1$) to intermediate ($0.1 < \lambda_b < 100$) blood solubility. This effort stemmed from the solubilities of the respiratory gases (partition coefficient for O_2 is 0.7 and for CO_2 is 3). However, the lungs exchange a wide variety of gases that range from low solubility, such as SF_6 or helium ($\lambda_b \approx 0.01$), to high solubility, such as water vapor ($\lambda_b \approx 20{,}000$–$50{,}000$, depending on temperature). The exchange of low- and intermediate-solubility gases occurs predominantly in the alveolar regions, with the airways providing a conduit for movement of gas between the alveoli and ambient air. In contrast, it is likely that the exchange of highly soluble gases ($\lambda_b > 100$), such as water vapor, occurs primarily within the conducting airways. However, highly soluble gas exchange with the pulmonary airways has not yet been fully characterized.

The absorption-excretion dynamics of a soluble gas are difficult to evaluate because of the relative inaccessibility of the airways to experimental measurements. Several previous investigators have attempted to describe the airway interaction of a variety of gases with a wide range of water solubilities (1, 1a, 25). In each of these studies, the dynamics of gas exchange with the airways are inferred after measurement of inlet and outlet concentration profiles. These studies confirm that soluble gases interact with the airways; however, many details of the exchange dynamics have not been described. For example, gases excreted in the alveoli via the pulmonary circulation can be reabsorbed in the mucous layer of the conducting airways (9). The resulting redistribution of the gas within the lung may have important ramifications to the excretion and/or metabolic kinetics of the gas.

A one-dimensional model of the airways previously developed in this laboratory describes the simultaneous exchange of heat, water, and a highly soluble gas with the pulmonary airways. Ethyl alcohol is the soluble gas used in the model simulations because of its high water and blood solubility ($\lambda_b = 1{,}756$) and its important applications in the medicolegal arena. The performance of the model was compared with exhaled axial profiles of air temperature available in the literature (27) and was subsequently used to quantify the relative contributions of the pulmonary and bronchial circulations, as well as each airway generation, to the net amount of soluble gas excreted with each breath. The effects of ventilatory rate, mode (nasal vs. oral) of breathing, and inspired air temperature and relative humidity have also been described (28). In each of these cases, steady-state tidal breathing was simulated.

The breathing profile used in breath alcohol testing is a transient full inhalation and single-exhalation maneuver. After quiet tidal breathing, the subject inhales a "deep breath," hopefully to total lung capacity (TLC), then exhales in a prolonged continuous fashion, hopefully to residual volume (RV). The accuracy of the single-exhalation breathing maneuver to determine blood alcohol concentration (BAC) is controversial, as the interaction of alcohol with the airways has not been characterized. In addition, the ventilation parameters (i.e., pretest breathing rate, inhaled and exhaled vol-

umes, and exhalation flow rate) that characterize the single-exhalation maneuver are poorly controlled in routine breath testing. For example, if the interaction of alcohol with the airways were sensitive to exhalation flow rate, then the concentration of alcohol arriving at the mouth would also depend on exhalation flow rate. Thus, it is important to develop a method that accurately describes the interaction of alcohol with the airways and predicts the effects of variable ventilation parameters. The purpose of this paper is to compare the performance of the model with experimentally measured single-exhalation alcohol profiles from human subjects. In doing so, we further validate the model as a means of describing highly soluble gas exchange with the pulmonary airways.

MATERIALS AND METHODS

Lung model. The mathematical model is described in detail elsewhere (27). Only the salient features are discussed here. The airways are divided radially into four regions: *1*) the airway lumen; *2*) a thin layer of mucus; *3*) a nonperfused tissue layer that represents the respiratory epithelium, basement membrane, and any connective tissue; before reaching *4*) the capillary bed of the bronchial circulation. Axially, the model has a symmetric bifurcating structure through 18 generations. The respiratory bronchioles and alveoli are lumped together as a single respiratory unit. Dimensions for the upper respiratory tract were taken from Hanna and Scherer (5), and those for the lower respiratory tract were from Weibel (29).

The air is considered a system of dry air, water vapor, and a single soluble gas. The very small exchange of respiratory gases with the airways is considered negligible. Temperature and concentration values in each region are bulk averages for the entire region. The gas is assumed to behave ideally, and longitudinal convective or diffusive mixing is neglected. Heat and mass transfer coefficients are used to describe the transport of heat and mass between the air and the mucous layer. The values are determined from empirical correlations (5, 10). The mucous and tissue layers are treated as dilute binary mixtures of water and a soluble gas. Both layers are assumed to have the physical properties of water. Filtration and diffusion (Fick's law) are the transport processes for water and the soluble gas between the capillary bed, tissue, and mucous layers. A variable mucous layer thickness is incorporated into the model to account for local hydration and dehydration. The resulting eight hyperbolic differential equations are solved numerically using a VAX station 3200 computer (VMS version 5.3). The spatial derivatives are handled with upstream finite differencing, whereas the time derivatives are solved using LSODE, a time-integration software package developed by A. Hindmarsh in 1981.

Subjects. Six male volunteers without previous history of cardiac or pulmonary disease and with normal physical examination findings served as subjects. Characteristics of the subjects are summarized in Table 1. The protocol was approved by the Washington Human Subjects Review Committee, and written informed consent was obtained from each subject. Each subject arrived at the laboratory without food consumption for the previous 4 h and without alcohol consumption for the previous 24 h. The subject's height, weight, and vital capacity were recorded. Each subject ingested enough alcohol in the form of liquor to achieve a BAC of ~0.09 g/100 ml, according to the Widmark (30) formula. After ingestion of the alcohol, the subjects waited ~1 h for absorption to take place. Absorption was monitored by sequential breath tests; the postabsorptive state was determined by three successively decreasing readings.

TABLE 1. *Subject characteristics*

Subj No.	Age, yr	Weight, kg	Vital Capacity, ml	Alcohol Dose, oz
1	48	102	6,000	8
2	24	86	5,200	6
3	22	73	6,000	6
4	33	70	4,400	6
5	26	63	4,600	5
6	27	75	6,000	6
Mean ± SD	30±10	78±14	5,400±740	6±1

Experimental materials. Alcohol concentration in the exhaled breath was measured with a commercially available infrared absorption breath testing instrument (Intoxilyzer 5000). After passing through the Intoxilyzer 5000, the exhaled breath entered a wedge spirometer where exhaled volume and flow rate were measured. The analog signals from the Intoxilyzer 5000 and wedge spirometer were sampled at a rate of 50 Hz using a commercially available data acquisition software package (Strawberry Tree) and a Macintosh IIcx. Figure 1 is a schematic of the experimental apparatus. The Intoxilyzer 5000 was calibrated with a breath alcohol simulator (Smith & Wesson Mark IIA) at a constant temperature of 34°C. The concentration of alcohol in the alcohol-water mixture was determined by gas chromatography using headspace analysis (11).

Experimental protocol. Each subject performed two different breathing maneuvers, each repeated five times. The first maneuver was a single inhalation to TLC followed by exhalation at a slow constant flow rate to RV (*maneuver A*). The second maneuver was identical to the first except exhalation was at a rapid constant flow rate (*maneuver B*). Each maneuver was spaced by ~3 min of quiet nasal tidal breathing, and the order of the maneuvers was alternated. Blood samples were taken from the antecubital vein at three points in time after the estimated start of the postabsorptive phase. BAC was subsequently measured with a gas chromatograph (Perkin-Elmer model 3920) using headspace analysis (11) and plotted against time for each subject (Fig. 2). The first data point for *subject 6* was discarded (as well as the breathing maneuvers performed before the 2nd data point) as the postabsorptive phase clearly had not been reached. A line was regressed through the remaining data points so that an estimate of the BAC at any point in time could be made for each subject.

RESULTS

Experimental results. The alcohol dose for each subject is listed in Table 1. The mean rate of decline in BAC in the postabsorptive phase for all subjects was 0.013 ± 0.0038 (SD) $g \cdot 100\ ml^{-1} \cdot h^{-1}$, and the mean Widmark

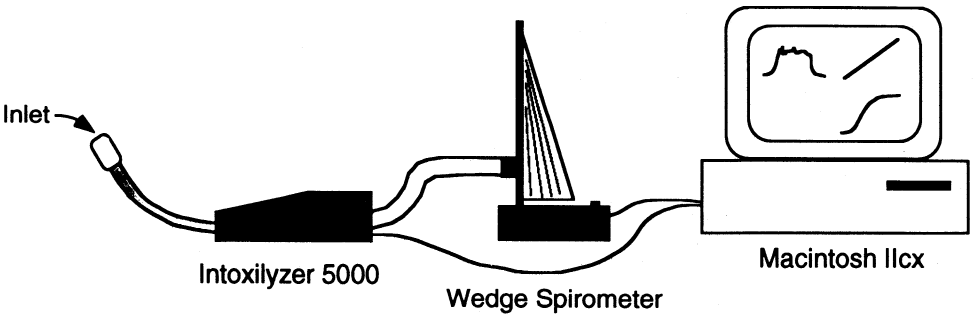

FIG. 1. Experimental setup used to collect exhaled alcohol profiles. Analog signal from Intoxilyzer 5000 and wedge spirometer was sampled at 50 Hz by Macintosh IIcx.

(30) r value was 0.67 ± 0.067 (SD). The Widmark r value represents the ratio of the whole body alcohol concentration to the BAC and is defined by the following relationship

$$r = \frac{C \cdot B \cdot G}{W(BAC + bt)} \quad (1)$$

where C is the concentration of alcohol in the beverage, B is the amount of beverage consumed (oz), G is the specific gravity of alcohol (0.789 g/ml), W is the subject's body weight (oz), b is the alcohol burn-off rate ($g \cdot 100\ ml^{-1} \cdot h^{-1}$), and t is the time from the start of beverage consumption (h).

Mean exhaled volumes and flow rates for each of the six subjects are summarized in Table 2. One trial from *subject 3, maneuver A*, was not included in the analysis as the exhaled volume was greater than two standard deviations from the mean. The flow rate of *maneuver B* was statistically ($P < 0.005$) greater than *maneuver A* when data for all six subjects were combined, as well as in each individual subject.

A simple smoothing routine (average of 10 nearest neighbors) was performed on each BAC profile. The y-axis was converted from BAC in grams per 100 ml to a mole fraction of alcohol in the exhaled air and then normalized by the mole fraction of alcohol in the alveoli. The normalized mole fraction of alcohol in air is given the symbol Y. The alveolar alcohol concentration is calculated from the BAC and λ_b (g alcohol · 100 ml blood^{-1} · g alcohol^{-1} · 100 ml air). The air is assumed to equilibrate with pulmonary capillary blood, and λ_b is calculated based on a hematocrit that is 80% of the systemic hematocrit. The hematocrit of the pulmonary microcirculation is difficult to assess. A variety of indirect techniques have been used, including morphometric measurements and volume dilution of indicators. The consensus is that the hematocrit of the pulmonary microcirculation is ~80% of the systemic hematocrit (18). Because the solubility of alcohol in red blood cells is significantly less than in plasma, hematocrit is an important variable in the determination of λ_b. The partition coefficient for alcohol and systemic blood (hematocrit 44.3%) and for alcohol and plasma at 37°C is 1,756 and 2,022, respectively (11). Assuming that the hematocrit of our subjects was ~44.3% and that there is a linear relationship between λ_b and the hematocrit, a partition coefficient of 1,810 between alcohol and blood in the alveoli is calculated.

The resulting profiles (Fig. 3) have three distinct phases. Phase I represents the delay in the rise of alcohol concentration as the volume of dead space is emptied. Phase II is the transition from dead space to exchange space, and phase III represents the emptying of the exchange space. In the case of a highly soluble gas such as

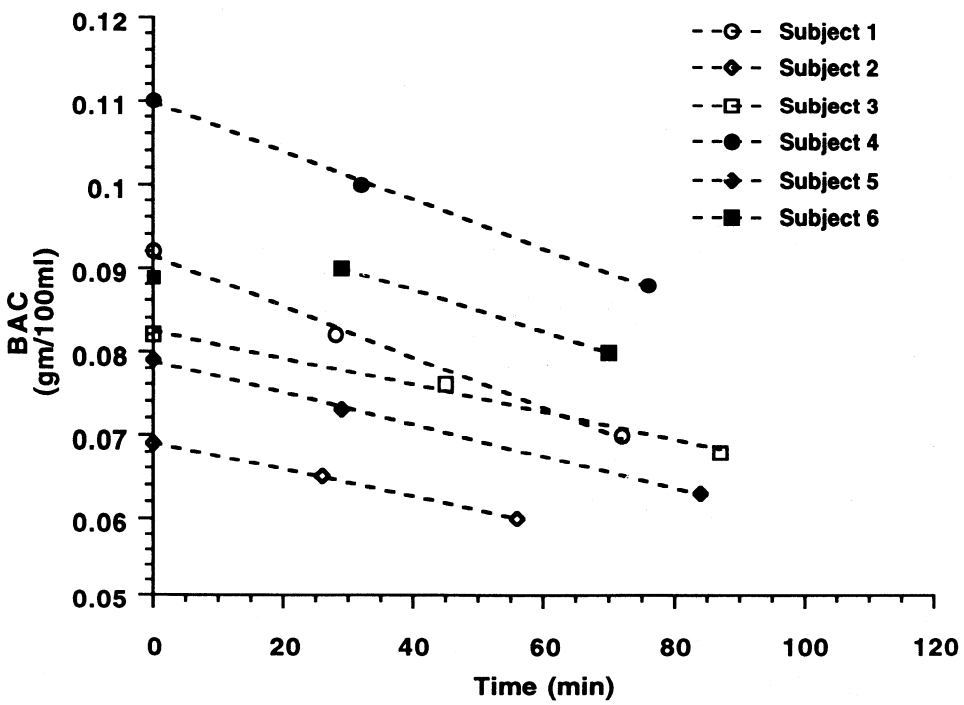

FIG. 2. Blood alcohol concentration (BAC) vs. time for all 6 subjects. Regression lines for each subject are shown. First point for *subj 6* was not included in regression.

TABLE 2. *Exhaled volumes and flow rates*

Subj No.	Maneuver	*n*	Exhaled Volume, ml	Flow Rate, ml/s
1	*A*	5	5,100±180	210±21
	B	5	5,700±250	450±37
2	*A*	5	3,700±420	320±39
	B	5	3,300±280	410±19
3	*A*	4	4,200±180	150±24
	B	5	4,600±200	280±37
4	*A*	5	3,500±100	140±11
	B	5	4,100±100	300±28
5	*A*	5	4,400±180	230±8
	B	5	4,500±83	350±8
6	*A*	3	5,600±85	160±5
	B	3	5,400±68	250±9
Mean ± SD	*A*	27	4,400±810	200±68
	B	28	4,600±870	340±78

n, no. of trials.

alcohol, the air in the conducting airways will contain alcohol and is thus considered part of the exchange space. Phase I in Fig. 3 represents the emptying of the RV of air that remains in the Intoxilyzer 5000 before the beginning of the exhalation and, therefore, does not represent part of the exhaled profile. Phase I was subsequently removed from each trial (range 60–150 ml). Next, each trial was truncated to the smallest exhaled volume within a subject. For example, the smallest exhaled volume within the 10 trials of *subject 1* was 4,930 ml; therefore, the data for the remaining 9 trials were truncated to 4,930 ml. In this manner, differences in exhaled volumes were not a confounding variable. Each group of profiles within a subject and maneuver type was subsequently condensed into a single representative exhalation maneuver by averaging the normalized alcohol concentration in the exhaled air at intervals of one-tenth total exhaled volume (Fig. 4). Condensing the profiles dramatically reduces computer simulation time, as 60 single-exhalation profiles have been reduced to 12 [6 subjects × 2 different maneuvers (*A* and *B*)].

Model results. Before a single-exhalation maneuver is simulated, the model must simulate 30 tidal breaths to reach steady-state conditions for temperature and concentration profiles in the airway lumen, mucous, and tissue regions (28). A respiratory rate of 12 breaths/min and a tidal volume approximated as 10% of the subject's vital capacity (6) were used. For all simulations, inspired air temperature was 23°C and relative humidity was 50%. Inspired volume, expired volume, and exhalation time must be specified to simulate the 12 condensed single-exhalation maneuvers. Inspired volume was determined on the basis of the assumption that each subject inhaled to TLC; inspired volume can then be approximated as 65% of the subject's vital capacity (6). Expired volume was determined as described above. The exhalation time for each condensed single-exhalation maneuver can be determined by dividing the expired volume by the mean flow rate of each group of maneuvers before the removal of phase I.

There are three distinct differences between the model's prediction and the experimental data (Fig. 4) that are consistent across maneuver type and subject: *1*) the model predicts a more rapid rise in alcohol concentration during phase II, *2*) the model predicts a smaller slope of phase III (S_{III}; calculated from a linear regression fit over the 2nd half of exhalation), and *3*) the model predicts a higher maximum alcohol concentration in the air at end exhalation. The model's prediction can be improved dramatically by reducing the molecular diffusion coefficient (D) of alcohol in the nonperfused tissue layer (Fig. 4). For each of the 12 condensed profiles, an optimal diffusion coefficient (D_{opt}) was determined to the nearest whole percent of the diffusion coefficient of alcohol in water (D_{H_2O}) by the method of least squares. Table 3 summarizes the D_{opt}, S_{III} (mol alcohol in air · mol alcohol in alveolus^{-1} · l^{-1}), normalized alcohol concentration at end exhalation (Y_{max}), root mean square error (RMS) for each condensed maneuver, and the model's prediction using D_{opt}. There is no statistical ($P > 0.05$) difference between *maneuver A* and *maneuver B* for any of the variables presented in Table 3. D_{opt} for all six subjects was 12×10^{-7} cm^2/s, which is 8% of D_{H_2O}. S_{III} is statistically

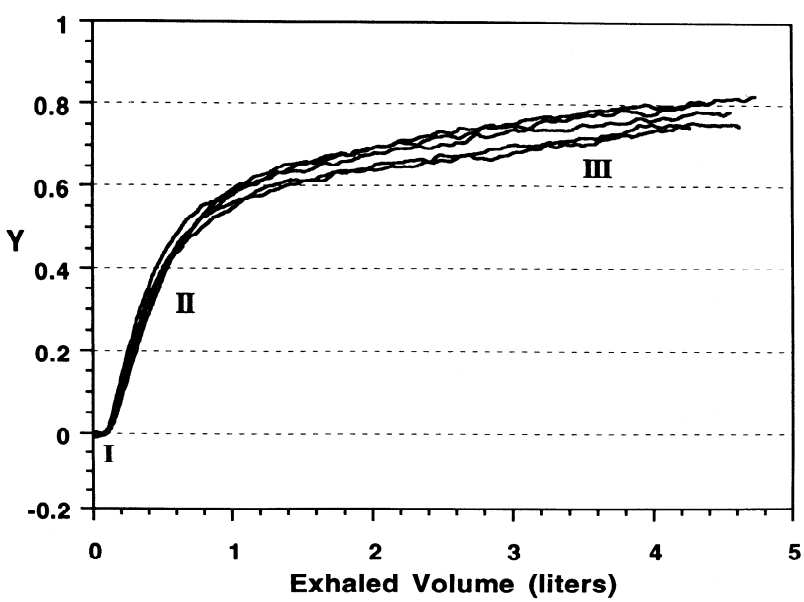

FIG. 3. Five exhaled alcohol profiles for *subj 5, maneuver A*. Phases I, II, and III are labeled. Phase I represents dead space of Intoxilyzer 5000 and was removed before analysis. Y, normalized mole fraction of alcohol in air.

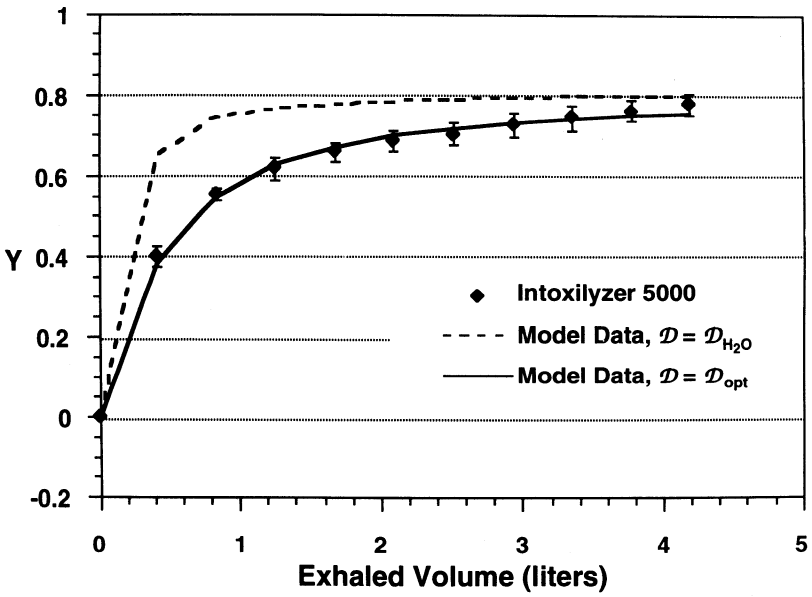

FIG. 4. Condensed exhaled profile for *subj 5, maneuver A* is shown with model's prediction using 2 values for diffusion coefficient (D) of alcohol in nonperfused tissue layer: alcohol in water (D_{H_2O}) and optimal value for D (D_{opt}) based on least squares. Each point in condensed profile represents mean of 5 corresponding points in Fig. 3 at increments of 1/10 of total exhaled volume. Error bars, ±SD.

significant ($P < 0.001$) for all maneuvers and subjects and has a mean value of 0.047 mol alcohol in air · mol alcohol in alveolus^{-1} · l^{-1}. The model prediction for S_{III} is 8.5% smaller than the S_{III} of the data, but this difference is not significant ($P > 0.05$). The mean Y_{max} is 72% of the alveolar concentration. The model prediction for Y_{max} is 1.4% larger than Y_{max} of the data but, again, is not significant ($P > 0.05$).

The model has been used previously to demonstrate that alcohol arriving at the mouth after a tidal breath comes primarily from the mucous layer rather than from the alveoli (28). To briefly summarize, as ambient air enters the airways on inspiration, it absorbs alcohol from the mucous layer in a bimodal axial distribution until reaching approximately the 12th-15th generation (depending on mode of breathing and flow rate) where the air reaches equilibrium with the mucus. As the air enters the alveoli, the model predicts that there is an additional flux of alcohol into the air. This additional flux of alcohol is due to the structure of the model at the transition from the terminal bronchioles to the respiratory bronchioles and alveoli. The model assumes an abrupt change from an air-water interface in the conducting airways to an air-blood interface in the alveoli. Alcohol is ~15% less soluble in the blood of the pulmonary microcirculation than in water, and this accounts for the higher concentration in the gas phase of the alveoli compared with the airway lumen. There is a large flux of alcohol from the airway back to the mucus immediately on the air exiting the alveoli. Over the course of exhalation, an average of ~25% of the alcohol in the alveoli redeposits on the mucous layer. The result is threefold: *1*) a bimodal distribution of net alcohol flux as a function of airway generation; *2*) 85% of the alcohol that arrives at the mouth is from the bronchial circulation, and the remaining 15% is from the pulmonary circulation; and *3*) 25% of the alcohol in the alveoli is redistributed in a characteristic fashion along the mucous layer where it acts to retard the excretion of alcohol from the bronchial circulation. The model can be used to make similar predictions for a single-exhalation maneuver using D equal to D_{H_2O}, as well as a reduced D.

The simulation parameters used to determine the distribution of the net flux of alcohol from the airways are

TABLE 3. *D_{opt}, S_{III}, Y_{max}, and RMS error of model*

Subj No.	Maneuver	D_{opt}	S_{III} (Data)	S_{III} (Model)	Y_{max} (Data)	Y_{max} (Model)	RMS
1	*A*	4.8	0.040*	0.042*	0.66	0.71	0.044
	B	4.8	0.037*	0.053*	0.63	0.69	0.038
2	*A*	9.6	0.061*	0.078*	0.66	0.69	0.028
	B	8.0	0.058*	0.092*	0.64	0.67	0.026
3	*A*	14	0.041*	0.032*	0.74	0.75	0.030
	B	13	0.042*	0.037*	0.71	0.73	0.018
4	*A*	24	0.061*	0.032*	0.81	0.77	0.018
	B	13	0.052*	0.045*	0.76	0.73	0.021
5	*A*	16	0.045*	0.028*	0.78	0.76	0.012
	B	11	0.040*	0.036*	0.74	0.74	0.012
6	*A*	13	0.042*	0.023*	0.80	0.77	0.024
	B	11	0.041*	0.024*	0.77	0.75	0.021
Mean ± SD	*A*	14±6.6	0.049±0.010	0.039±0.020	0.74±0.067	0.74±0.033	0.026±0.011
	B	10±3.1	0.045±0.0083	0.048±0.024	0.71±0.060	0.72±0.030	0.023±0.0090
	A&B	12±5.3	0.047±0.0089	0.043±0.022	0.72±0.063	0.73±0.032	0.024±0.010

D_{opt}, optimal diffusion coefficient ($\times 10^7$ cm^2/s); S_{III}, slope of phase III (mol alcohol in air · mol alcohol in alveolus^{-1} · l^{-1}); Y_{max}, concn of alcohol at end expiration (normalized); RMS, root mean square error. * Statistically different from 0 using Student's t test ($P < 0.001$).

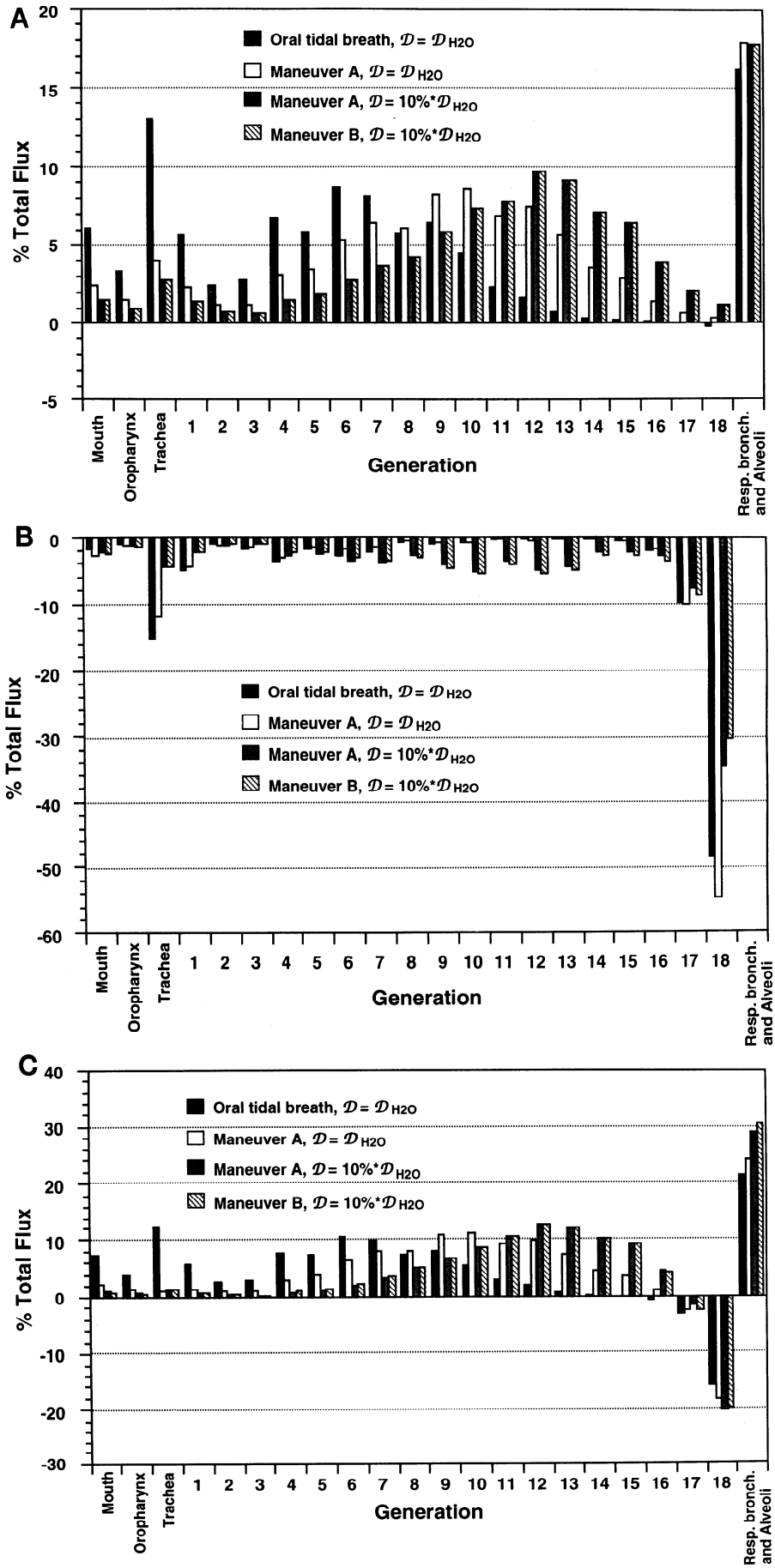

FIG. 5. *A*: axial distribution of alcohol flux on inspiration as predicted by model using value for D of alcohol in tissue that is 10% of D_{H_2O}. *B*: axial distribution of alcohol flux on expiration as predicted by model using value for D of alcohol in tissue that is 10% of D_{H_2O}. *C*: net (inspiration + expiration) axial distribution of alcohol flux as predicted by model using value for D of alcohol in tissue that is 10% of D_{H_2O}. Tidal breathing, single exhalation, tissue diffusivity of alcohol, and expiratory flow rate are contrasted. Positive flux denotes mucus to air; negative flux denotes air to mucus. Resp bronch, respiratory bronchioles.

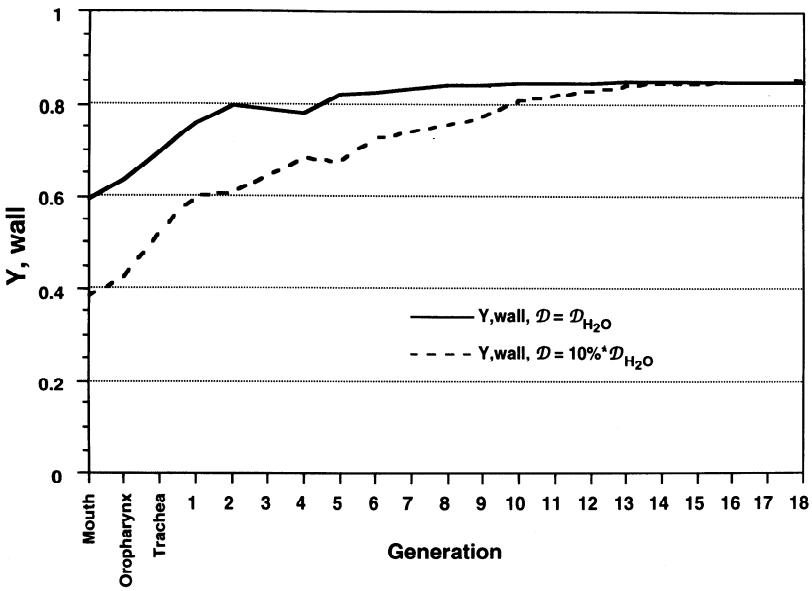

FIG. 6. Axial distribution of normalized concentration of alcohol in equilibrium with mucous layer before single-exhalation maneuver (Y, wall). Data for D_{H_2O} and 10% D_{H_2O} are presented.

based on the mean vital capacity of the six subjects, the mean flow rate for *maneuver A* and *B*, and either D_{H_2O} or a D that is 10% of D_{H_2O}. Figure 5 demonstrates the progressive changes in the axial distribution of alcohol flux to (negative) and from (positive) the mucus during inspiration and expiration and the net distribution for an oral tidal breath, a single exhalation, a single exhalation with reduced D, and a single exhalation with reduced D and a high exhalation flow rate.

On inspiration (Fig. 5*A*), there is a bimodal distribution with peaks in the trachea and sixth generation for the oral tidal breath. The decreasing flux between the trachea and the second generation is due to the decreasing driving force for flux of alcohol from the mucus to the air. The rise in flux to the second peak is due to the rapid increase in surface area available for alcohol flux as the airways progressively bifurcate. The initial peak for the single-exhalation maneuver remains but is reduced in magnitude relative to the tidal breath. The second peak is shifted toward the alveoli to 10th generation, and the air does not quite reach equilibrium with the mucus before entering the alveolar region. The model uses the same inspiration time for a tidal breath and a single exhalation; therefore, the flow rate for the single-exhalation maneuver is larger than for the tidal maneuver. The increased flow rate on inspiration in the single-exhalation maneuver accounts for the changes in the inspiratory flux distribution (Fig. 5*A*) by the following argument. The rapid flow rate increases the mass transfer coefficient to the one-third power but decreases the residence time available for transfer to the first power. Thus the net effect is to delay (or shift flux distribution toward the alveoli) the flux of alcohol. Reducing D acts to further decrease the magnitude of the initial peak, as well as shift the second peak further toward the alveoli (12th generation). The mechanism accounting for these effects is relatively simple. The steady-state axial concentration profile of alcohol in the mucous layer, which determines the magnitude for axial flux, is altered (Fig. 6). The concentration of alcohol in the mucus in the upper respiratory tree is reduced. This difference is compensated for by a steep positive gradient between the 3rd and 12th generations, corresponding exactly to the rise in alcohol flux, leading to the shifted second peak. The changes seen in the axial mucous concentration profile are due to enhanced recovery of alcohol on exhalation and are addressed below in the discussion of Fig. 5*B*. As expected, there is no difference in the inspiratory flux profiles between slow and rapid exhalation flow rates.

There are three characteristics of the expiratory flux profiles seen in Fig. 5*B* that deserve mention. The first is the large negative flux (air to mucus) in 18th generation as the air exits the alveoli and encounters the air-water interface. The flux in the 18th generation accounts for between 31 and 54% of the total negative flux. This large flux is mainly attributed to the change from an air-blood interface in the alveoli to an air-water interface in the airways and serves to balance the large positive flux in the alveoli seen in the inspiratory flux profiles (Fig. 5*A*). The second observation is the reduced percentage of alcohol recovered in the 18th generation when D is reduced (54 to 34%). A portion of this reduction can be attributed to a higher absolute concentration of alcohol in the mucus (thus a smaller driving force for alcohol flux) in the 18th generation (Fig. 6). The remainder is accounted for by the final result: an increased recovery of alcohol in the 7th–15th generations, leading to a larger total amount of alcohol recovered. When a D equal to D_{H_2O} is used, 26% (24% for a tidal breath) of the alcohol in the alveoli is reabsorbed by the airways over a complete exhalation; this increases to 40% (44% for a tidal breath) when the tissue diffusivity is reduced by 10-fold. Reducing D enhances the airways' ability to recover alcohol on expiration. The driving force for recovery of alcohol is a pressure gradient between the air and mucus. Reducing the diffusing capacity (D) of alcohol in the tissue layer effectively hinders the tissue layer's ability to replenish the alcohol (from the bronchial circulation) that the mucous layer lost to the air on inspiration. Hence, as exhalation begins, the air encounters a mucous layer in which the alcohol pressure is less than it would be for the case of a larger tissue diffusivity. The more distal airways are able to recover alcohol more efficiently, thus accounting for the findings in Figs. 5*B* and 6. The shift in alcohol

recovery toward the mouth in the rapid exhalation flow rate is caused by the same effect described earlier in the case of differing inhalation flow rates (i.e., mass transfer coefficient vs. residence time).

The net flux (inspiration plus expiration) profile in Fig. 5*C* is useful to demonstrate several points. The first is the near obliteration of the net positive flux in the upper respiratory tree when a single-exhalation maneuver is performed. This is due to the reduced contribution of the upper respiratory tract on inhalation, as seen in Fig. 5*A*. The contribution of the alveolar space to the net alcohol loss is approximately twice as large as any individual airway generation and ranges from 22 to 31% of the total alcohol loss. There exists a point along the respiratory tree where all of the alcohol absorbed by the air on inspiration is redeposited to the mucus on expiration. This point varies from between the 14th and 15th generation to between the 16th and 17th generation depending on the breathing maneuver and the tissue diffusivity of alcohol. Generations to the left (toward the mouth) of this point have a net positive flux and those to the right (toward the alveoli) have a net negative flux.

The mathematical model is able to predict the experimental data and, in doing so, suggests a reduced D of alcohol in tissue relative to D_{H_2O}. In addition, the model predicts that the vast majority of alcohol exchange occurs within the conducting airways and not the alveoli. The interaction of alcohol with the airways can subsequently be used to explain the shape of the exhalation profile.

DISCUSSION

Reduced D in tissue. It is likely that the diffusivity of alcohol through organized cellular tissue is less than the diffusivity of alcohol through water. Over 40 years ago Kety (15) estimated that the D values of gases in tissue were between 30 and 50% of their diffusivities in water. The first study to investigate the permeability of alcohol in tissue was reported in 1969 by Chinard et al. (2). The study compared the relative diffusivities of a series of monohydric alcohols (methanol to hexanol) to tritiated water using the indicator-dilution technique in the kidney. They were able to demonstrate that increasing alkyl chain length, and therefore increasing lipid solubility, increased the ratio of alcohol diffusivity in tissue to alcohol diffusivity in water. In other words, increasing lipid solubility increased the diffusivity of the solute in tissue. The ratio D/D_{H_2O} was never greater than 1 and had a range of 0.33–0.72 for ethanol. A limitation of this technique is that only relative D can be calculated. Also, this technique measures relative D of whole tissue with heterogeneous cell types.

Studies by Polefka et al. (22) and Garrick and Chinard (3) utilized a different technique to measure the permeability of the cell membrane to a similar series of monohydric alcohols at 37°C. Garrick and Chinard used a collection of pulmonary cells (65% type II alveolar cells; 20% macrophages; and the remainder a mix of endothelial cells, type I alveolar cells, and monocytes), whereas Polefka et al. used a cell line derived from a hepatoma. The cells were tightly packed by centrifuge into a cylindrical column, and radiolabeled alcohol was allowed to diffuse into the semi-infinite mass of cells for a known amount of time. The permeability of the cells used by Garrick and Chinard was 3.58×10^{-3} cm/s. If one assumes the average diameter of a cell is 10 μm, D is 3.58×10^{-6} cm^2/s or 22% of alcohol in water. Similar analysis of the data from Polefka et al. gives a D of 2.32×10^{-6} cm^2/s for the hepatoma cells, which is 15% of alcohol in water.

Two factors can explain the reduced diffusivity of alcohol in tissue reported by these studies and confirmed by our model: *1*) increased viscosity of the cytoplasm and *2*) relatively poor lipid solubility of alcohol. A variety of techniques and molecules have been used to measure D of the cytoplasm, and the results have been relatively consistent. It is now well accepted that small molecules, such as alcohol, have a D in cytoplasm that is between 20 and 50% that in water (16, 20) and is inversely related to molecular size. This decrease is presumably due to the presence of proteins, inorganic ions, sugars, and metabolites that act to increase the viscosity of the cytoplasm by two to six times that of water. As alcohol is smaller than the molecules in the cytoplasmic studies, one would expect the diffusivity of alcohol in the cytoplasm to be a minimum of 50% that in water. Alcohol is nearly 15 times less soluble in lipid than in water (2). Therefore, the lipid bilayer of the cell would be expected to offer substantial resistance to the movement of alcohol. This is confirmed in the results reported by Garrick and Chinard and Polefka et al., who attribute 32 and 72%, respectively, of the total resistance to the D of alcohol across a cell to the cell membrane.

Although the results of these previous studies are consistent with our model's prediction of a reduced diffusivity of alcohol in tissue relative to water, the values they attained (range 15–72% of D_{H_2O}) are all larger than our model's prediction (8% of D_{H_2O}). A mathematical model of this magnitude requires many simplifying assumptions, many of which can impact the shape of the exhalation profile and, hence, our model's prediction of D_{opt}. Assumptions regarding the surface area available for diffusion, the solubility of alcohol in tissue, and the thickness of the tissue and mucous layers, as well as other factors such as asymmetric airway branching, Taylor diffusion, lumping the radial concentration profile into two compartments, and a finite bronchial capillary blood flow, may all play a role in explaining the discrepancy between our model's prediction for D of alcohol in tissue and that measured experimentally.

The D of alcohol in the tissue layer is defined by the following expression

$$\mathrm{D} = \frac{D\beta_t A}{L_t} \tag{2}$$

where β_t is the solubility of alcohol in tissue (ml alcohol · ml tissue^{-1} · mmHg^{-1}), A is the surface area available for diffusion, and L_t is the thickness of the tissue. Reducing D of alcohol in the tissue layer acts to reduce D of the tissue. A reduced D in the model creates the desired improvement of the fit to the experimental data. It can be seen from *Eq. 2* that a similar effect can be achieved by decreasing either A or β_t or increasing L_t.

The capillary bed of the bronchial circulation is comprised of a dense microvascular network (17). In con-

trast, our model assumes a continuous capillary sheet. The A available for diffusion from the capillary bed to the nonperfused tissue layer in each airway generation is calculated from the length and diameter of that generation as reported by Weibel (29). It is difficult to quantify A of the capillary bed, but the assumption of a continuous capillary sheet produces a maximum value. This may account for an overestimation of D in the original model and a subsequent underestimation of the fitted diffusion coefficient, D_{opt}.

Because alcohol is relatively hydrophilic, water content is the most important factor determining solubility. The water content of blood is a function of hematocrit and has a mean value of 79% for men and 81% for women (11). In general, the water content of tissue is less than that of blood and ranges from 74% in muscle to 77% in the kidney (13). The water content of lung tissue is expected to be similar. Therefore the solubility of alcohol in lung tissue is expected to be ~5% lower than in blood. The model assumes that the solubility of alcohol in tissue is equal to that of alcohol in blood. As is the case for A, this assumption may produce an overestimation of D and a subsequent underestimation of D_{opt}.

The values of L_t used by the model are larger than the thickness of the respiratory epithelium by light microscopy (4) at every point in the respiratory tree. This increase is to account for any connective tissue that lies between the capillary bed and epithelium, which the model incorporates into L_t. As D was reduced by >12-fold, a similar increase in L_t would be required to produce the same effect. The values for L_t are already exaggerated, and any further increase would be unrealistic.

The D of the mucous layer also impacts the shape of the exhalation profile. However, this impact is much smaller relative to the D of the tissue layer because the thickness of the mucous layer (L_m) is ~50 times smaller than L_t. Increasing L_m will improve the fit of the model to the experimental data by decreasing D of the respiratory mucosa, as well as enhancing the recovery of alcohol on exhalation by providing a larger reservoir for deposition. However, the value of L_m used by the model is 10 μm, which is the maximum that can be found in the literature (19). Therefore, as in the case of L_t, increasing L_m in the model is unwarranted.

Asymmetric branching of the airways would likely impact the convective mixing of the gas in the airways. This may affect the exchange of gases with low solubility, the exhalation profile of which depends on the relative convective and diffusive mixing that occur within the gas phase (23). However, this is unlikely to affect the profile of alcohol, which depends on the interaction with the airway wall. Kaye and Schroter (14) have recently demonstrated that as water solubility increases the effect of airway branching on the relative dispersion of a gas decreases. For acetaldelhyde, which is nearly 15 times less soluble than alcohol, airway branching had essentially no effect on gas dispersion.

Taylor diffusion has been invoked as an explanation for the separation of gases of different molecular weight and, hence, different gas phase diffusivity. Scheid and Piiper (23) concluded that Taylor diffusion plays only a very minor role in gas exchange theory. In addition, Kaye and Schroter (14) also demonstrated that increasing water solubility enhances Taylor diffusion, thus increasing the gas phase mixing within the airway lumen. Because of the large water solubility of alcohol, Taylor diffusion lends support to our assumption in the model of a well-mixed gas phase.

Approximating the radial concentration profile as two well-mixed compartments is a gross simplification but is valid when the relative resistance of convective mass transfer from the air is larger than diffusive resistance in the mucus and tissue. In this case, diffusion in the mucous and tissue layers is rapid relative to the delivery of gas by the airstream, resulting in a flat (i.e., well-mixed) concentration profile. Although reducing D of alcohol in tissue acts to increase the tissue resistance, it also shifts the gas exchange burden toward the alveoli (Fig. 5). Because the model scales L_t to the airway diameter, the tissue resistance decreases with increasing generation number. For the 9th–17th generations, the ratio of convective mass transfer resistance to tissue diffusive resistance ranges from 5 to 50, which supports the contention of a relatively flat concentration profile across the mucus and tissue.

Finally, the model assumes a constant BAC, in other words, an infinite bronchial capillary blood flow. The theoretical aspects of a combined perfusion- and tissue diffusion-limited system have been developed by Hlastala (8). The gas exchange kernel for such a system is

$$E = \frac{\lambda_b G}{\lambda_b G + \dot{V}_A/\dot{Q}} \qquad (3)$$

where E is the excretion (partial pressure of gas in the air leaving the exchange region normalized by the partial pressure in the incoming arterial blood), $G = 1 - \exp(-D/\dot{Q}\beta_b)$ (where β_b is the solubility of alcohol in blood), $\dot{V}_A$ is the alveolar gas flow rate, and $\dot{Q}$ is the blood flow rate. G is a term representing diffusion limitation within the tissue. Swenson et al. (26) demonstrated in an in vivo dog trachea that E of a gas from the bronchial circulation was a strong function of λ_b. The more soluble a gas, the larger the E. Acetone, the most soluble gas investigated in this study ($\lambda_b = 315$), was shown to equilibrate completely between the bronchial circulation and the air (E = 1.0). It is evident from *Eq. 3* that the larger λ_b (and hence solubility) is, the larger E is; hence, because alcohol is more soluble than acetone, its E is expected to be unity, also. In addition, *Eq. 3* demonstrates that E approaches unity as $\dot{Q}$ becomes infinite. This is consistent with the model's assumption of an infinite capillary blood flow.

Alveolar concentration of alcohol. The results have been presented based on a microcirculatory hematocrit that is 80% of the systemic hematocrit ($\lambda_b = 1{,}810$). The experimental data have also been analyzed using $\lambda_b = 1{,}756$, i.e., a pulmonary microcirculation hematocrit that is equal to the systemic hematocrit (Fig. 7). Reducing λ_b by 3% (1,810 to 1,756) increases the concentration of alcohol in alveolar air relative to capillary blood by 3% for both the experimental data and the model prediction. Because the model prediction is shifted by the same fraction, D_{opt} is unchanged. The average S_{III} changes only modestly from 0.047 to 0.045 mol alcohol in air · mol alcohol in alveolus^{-1} · l^{-1}. The mean RMS error increases (fit of model

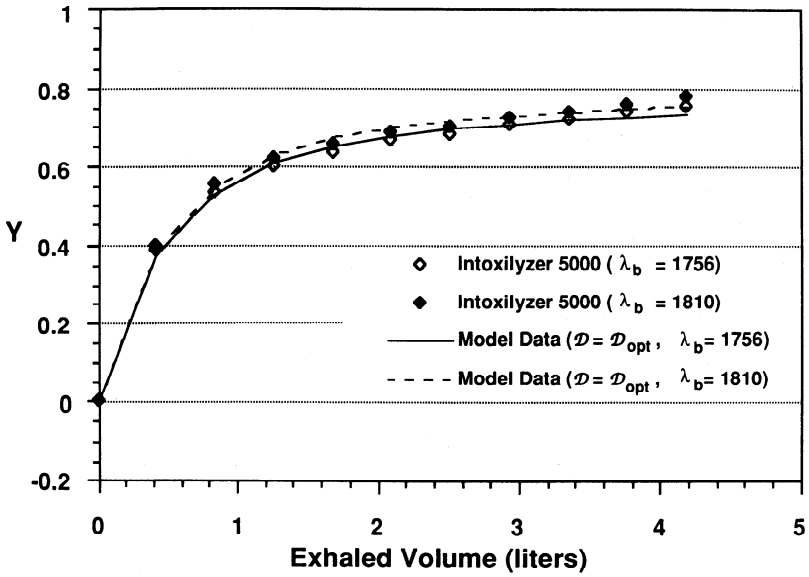

FIG. 7. Comparison of experimental and model data when blood-to-air partition coefficient (λ_b) is reduced from 1,810 to 1,756. Model data are presented using D_{opt}.

worsens) slightly from 0.024 to 0.025 when a λ_b of 1,756 is used.

In addition, rebreathing maneuvers provide indirect evidence consistent with the hematocrit of the pulmonary microcirculation being less than the systemic hematocrit. The concentration of alcohol in the alveoli cannot be directly measured; however, attempts have been made to improve the indirect sampling of alveolar air by rebreathing, which provides a breath sample that is closer to the true mixed alveolar air. Jones (12) demonstrated that progressive cycles of rebreathing produced higher breath alcohol concentrations than the single-exhalation maneuver. Consequently, the blood-to-breath ratio, which is equivalent to λ_b if a sample of true mixed alveolar air is attained, decreased from 2,225 to 1,947 after five cycles of rebreathing. Ohlsson et al. (21) also reported a decrease in the blood-to-breath ratio from 2,450 to 2,075 after six cycles of rebreathing. If the hematocrit of the pulmonary circulation were equivalent to the systemic hematocrit, the blood-to-breath ratio after rebreathing should approach 1,756, the value of λ_b for systemic blood. The fact that the blood-to-breath ratios after rebreathing are >1,756 supports the contention that the hematocrit of the pulmonary microcirculation is less than that of the systemic circulation.

S_{III}. S_{III} for a single exhalation can be explained by a reduced D of alcohol in the tissue layer and the subsequent effects on soluble gas exchange with the airways. We have discussed how the mucous layer, on inspiration, is stripped of alcohol by the incoming ambient air and very nearly reaches equilibrium with the mucus before entering the alveolar space. The reduced diffusivity of alcohol in the tissue layer hinders its ability to replenish the mucous layer. On exhalation, the air encounters a lower mucus concentration and therefore a larger driving force for the redeposition of alcohol on the mucus. The enhanced recovery of alcohol by the mucous layer delays the rise in alcohol concentration at the mouth, thus accounting for a steeper S_{III}. This mechanism of S_{III} represents a temporal heterogeneity of gas pressure within the exchange region and is inherently different from that described for lower solubility gases such as N_2 and CO_2.

Scheid and Piiper (23) introduced the concept of sequential emptying to explain the S_{III} of insoluble gases. Ventilation-volume and $\dot{V}A/\dot{Q}$ mismatching in the inhomogenous conducting airways and alveoli result in preferential emptying of regions in the lung with lower marker gas concentration. This mechanism represents a parallel heterogeneity of gas pressure within the exchange region and cannot be used to describe the S_{III} of a highly soluble gas such as alcohol. As air enters the alveolar space, it immediately equilibrates with the alcohol pressure of the blood. Because of alcohol's very large partition coefficient (λ_b = 1,756 at 37°C), a $\dot{V}A/\dot{Q}$ of >100:1 would be required to cause a significant reduction in the partial pressure of alcohol in the alveoli below that of the venous blood. In normal lungs, the physiological range of $\dot{V}A/\dot{Q}$ is 0.1–10; therefore, the partial pressure of alcohol in each alveoli is equal to the venous partial pressure. Even with the presence of sequential emptying, the pressure of alcohol in the gas leaving the alveoli would be constant.

More recently, Scherer et al. (24) demonstrated that a distributed alveolar region can explain the S_{III} during tidal breathing of gases with intermediate (CO_2) and low (SF_6 and He) solubility. This mechanism represents a serial heterogeneity of gas pressure in the exchange region. In other words, an intra-airway axial pressure gradient accounts for the positive S_{III}. Our model is similar in that there exists a distributed exchange region. In the case of alcohol this region occurs in the airways rather than in the alveoli. However, our explanation of the S_{III} applies to the single-exhalation maneuver where the exhaled volume is ~20 times larger than the volume of the exchange region. Hence, the positive S_{III} cannot be due to an intra-airway pressure gradient. Rather, the pressure of alcohol in the exchange region is spatially homogeneous relative to the temporal heterogeneity that results from the progressively decreasing flux of alcohol to the mucous layer during exhalation.

Alcohol flux distribution. Reducing the D of alcohol in the nonperfused tissue layer has a profound effect on the distribution of alcohol flux between the airway lumen and mucous layer. The contribution of the upper respiratory tree is significantly reduced as an overall shift toward the alveoli in alcohol flux is produced. Although not shown in Fig. 5*A*, the amount of alcohol arriving at the

mouth during oral tidal breathing that arises from the alveoli is essentially unchanged when D is reduced by 10-fold (16.3 to 15.4% of alcohol in the alveoli); however, the 83% increase in reabsorption by the mucous layer (24 to 44% of the alcohol in the alveoli) on exhalation has interesting ramifications. The increased reabsorption or deposition retards the movement of alcohol from the bronchial circulation to the airway lumen. Hence, a reduced D in the tissue layer hinders the lung's ability to excrete alcohol. This is relatively unimportant in the case of alcohol where the lung accounts for only 2–5% of the excretion (13). However, it seems reasonable that other highly soluble gases would have a reduced D in tissue also. If the lung played a significant role in their excretion, the model would predict an extended half-life.

Conclusions. A single-exhalation maneuver has been used to generate data on the exhalation profile of alcohol, a highly soluble gas. The profile has only phases II and III of the traditional profile, which describe low and intermediate solubility gases. Phase I no longer exists, as the "conducting" airways are now part of the exchange space. The experimental data are consistent with a D of alcohol in the respiratory mucosa that is 8% of that of D_{H_2O} as predicted by a mathematical model of highly soluble gas exchange with the pulmonary airways. The reduced diffusivity and the subsequent effect on highly soluble gas exchange can explain the S_{III} of a single-exhalation maneuver for a highly soluble gas. Finally, the reduced diffusivity enhances recovery of alcohol on exhalation, thus decreasing the excretion by the lung.

The authors especially thank Mical Middaugh and David Frazer for assistance in collecting the exhaled alcohol profiles. They also thank members of the Washington State Toxicologists Laboratory for gas chromatograph analysis of the blood and simulator liquid samples for alcohol concentration.

This work was supported in part by National Heart, Lung, and Blood Grants HL-24163 and HL-07403.

Address for reprint requests: M. P. Hlastala, Div. of Pulmonary and Critical Care Medicine, RM-12, Univ. of Washington, Seattle, WA 98195.

Received 10 August 1992; accepted in final form 16 July 1993.

REFERENCES

1. AHARONSON, E. F., H. MENKES, G. GURTNER, D. L. SWIFT, AND D. F. PROCTOR. Effect of respiratory airflow rate on the removal of soluble vapors by the nose. *J. Appl. Physiol.* 37: 654–657, 1974.

1a. BEN-JEBRIA, A., S.-C. HU, E. L. KITZMILLER, AND J. S. ULTMAN. Ozone absorption into excised porcine and sheep trachea by a bolus-response method. *Environ. Res.* 56: 144–157, 1991.

2. CHINARD, F. P., C. N. THAW, A. C. DELEA, AND W. PERL. Intrarenal volumes of distributions and relative diffusion coefficients of monohydric alcohols. *Circ. Res.* 25: 343–357, 1969.

3. GARRICK, R. A., AND F. P. CHINARD. Membrane permeability of isolated lung cells to nonelectrolytes at different temperatures. *Am. J. Physiol.* 243 (*Cell Physiol.* 12): C285–C292, 1982.

4. GASTINEAU, R. M., P. J. WALSH, AND N. UNDERWOOD. Thickness of the bronchial epithelium with relation to exposure to radon. *Health Phys.* 23: 857–860, 1972.

5. HANNA, L. M., AND P. W. SCHERER. Measurement of local mass transport coefficients in a cast model of the human upper respiratory tract. *J. Biomech. Eng.* 108: 12–18, 1986.

6. HILDEBRANDT, J. Structural and mechanical aspects of respiration. In: *Textbook of Physiology,* edited by H. D. Patton, A. F. Fuchs, B. Hille, A. M. Scher, and R. Steiner. Philadelphia, PA: Saunders, 1989, vol. 2, p. 991–1011.

8. HLASTALA, M. P. Diffusing capacity heterogeneity. In: *Handbook of Physiology. The Respiratory System. Gas Exchange.* Bethesda, MD: Am. Physiol. Soc., 1987, sect. 3, vol. IV, chapt. 12, p. 217–232.

9. HLASTALA, M. P., AND E. R. SWENSON. Airway gas exchange. In: *The Bronchial Circulation,* edited by J. Butler. New York: Dekker, 1992, vol. 57, p. 417–441. (Lung Biol. Health Dis. Ser.)

10. INGENITO, E. P., J. SOLWAY, E. R. MCFADDEN, AND J. M. DRAZEN. A quantitative study of heat transfer coefficients in the upper tracheobronchial tree of man (Abstract). *Federation Proc.* 45: 1020, 1986.

11. JONES, A. W. Determination of liquid/air partition coefficients for dilute solutions of ethanol in water, whole blood, and plasma. *J. Anal. Toxicol.* 7: 193–197, 1983.

12. JONES, A. W. Role of rebreathing in determination of the blood-breath ratio of expired ethanol. *J. Appl. Physiol.* 55: 1237–1241, 1983.

13. KALANT, H. Absorption, diffusion, distribution, and elimination of ethanol: effects on biological membranes. In: *The Biology of Alcoholism,* edited by B. Kissin and H. Begleiter. New York: Plenum, 1970, vol. 1, p. 1–62.

14. KAYE, S. R., AND R. C. SCHROTER. An experimental model of gas dispersion and uptake at the bronchial wall. *J. Biomech. Eng.* 115: 91–96, 1993.

15. KETY, S. S. The theory and applications of the exchange of inert gas at the lungs and tissues. *Pharmacol. Rev.* 3: 1–41, 1951.

16. KUSHMERICK, M. J., AND R. J. PODOLSKY. Ionic mobility in muscle cells. *Science Wash. DC* 166: 1297–1298, 1969.

17. LAITINEN, L. A., AND A. LAITINEN. The bronchial circulation: histology and electron microscopy. In: *The Bronchial Circulation,* edited by J. Butler. New York: Dekker, 1992, vol. 57, p. 79–106. (Lung Biol. Health Dis. Ser.)

18. LEE, J. S. Microvascular hematocrit of the lung. In: *Frontiers in Biomechanics,* edited by G. W. Schmid-Schoenbein. New York: Springer-Verlag, 1986, p. 353–364.

19. LUCHTEL, D. L. The mucous layer of the trachea and major bronchi in the rat. *Scanning Electron Microsc.* 2: 1089–1098, 1978.

20. MASTRO, A. M., M. A. BABICH, W. D. TAYLOR, AND A. D. KEITH. Diffusion of a small molecule in the cytoplasm of mammalian cells. *Proc. Natl. Acad. Sci. USA* 81: 3414–3418, 1984.

21. OHLSSON, J., D. D. RALPH, M. A. MANDELKORN, A. L. BABB, AND M. P. HLASTALA. Accurate measurement of blood alcohol concentration with isothermal rebreathing. *J. Stud. Alcohol* 51: 6–13, 1990.

22. POLEFKA, T. G., W. R. REDWOOD, R. A. GARRICK, AND F. P. CHINARD. Permeability of Novikoff hepatoma cells to water and monohydric alcohols. *Biochim. Biophys. Acta* 642: 67–78, 1981.

23. SCHEID, P., AND J. PIIPER. Intrapulmonary gas mixing and stratification. In: *Pulmonary Gas Exchange,* edited by J. B. West. New York: Academic, 1981, vol. 1, p. 87–130.

24. SCHERER, P. W., S. GOBRAN, S. J. AUKBURG, J. E. BAUMGARDNER, R. BARTKOWSKI, AND G. R. NEUFELD. Numerical and experimental study of steady-state CO_2 and inert gas washout. *J. Appl. Physiol.* 64: 1022–1029, 1988.

25. SCHRIKKER, A. C. M., W. R. DE VRIES, A. ZWART, AND S. C. M. LUIJENDIJK. Uptake of highly soluble gases in the epithelium of the conducting airways. *Pfluegers Arch.* 405: 389–394, 1985.

26. SWENSON, E. R., H. T. ROBERTSON, N. L. POLISSAR, M. E. MIDDAUGH, AND M. P. HLASTALA. Conducting airway gas exchange: diffusion-related differences in inert gas elimination. *J. Appl. Physiol.* 72: 1581–1588, 1992.

27. TSU, M. E., A. L. BABB, D. D. RALPH, AND M. P. HLASTALA. Dynamics of heat, water, and soluble gas exchange in the human airways. I. A model study. *Ann. Biomed. Eng.* 16: 547–571, 1988.

28. TSU, M. E., A. L. BABB, E. M. SUGIYAMA, AND M. P. HLASTALA. Dynamics of soluble gas exchange in the airways. II. Effects of breathing conditions. *Respir. Physiol.* 83: 261–276, 1991.

29. WEIBEL, E. *Morphometry of the Human Lung.* New York: Springler-Verlag, 1963.

30. WIDMARK, E. M. P. *Principles and Applications of Medicolegal Alcohol Determination (Die theoretischen Grundlagen und die praktische Verwendbarkeit der gerichtlichmedizinischen Alkoholbestimmung).* Davis, CA: Biomedical Publications, 1981.